Parameters' Effect on Weld Quality for Dissimilar Spot Welding Between Ferritic Stainless Steel and Low Carbon Steel Sheets

M. El-Shennawy[1] and S. M. Khafagy[2]

[1]Mechanical Engineering Department, Faculty of Engineering, Helwan University, Helwan, Cairo, Egypt
[2]Tabbin Institute for Metallurgical Studies (TIMS), P.O.B 109 Helwan, Cairo, Egypt.
E-mail: moha_111@yahoo.com; egtimsmmk@hotmail.com

Abstract: This work discusses the effect of main controlling parameters of spot welding process on the quality of dissimilar welded joint between ferritic stainless steel grade 430, FSS with 0.5 mm thickness and low carbon steel, LCS with 0.6 mm thickness sheets. Parameters studied were welding current, welding time and electrode pressure. Metallurgical and mechanical characteristics were determined through microstructure, tensile shear and microhardness examinations. The results of this study showed that the suitable electrode pressure in this dissimilar combination of steels; FSS and LCS; was 0.2MPa (2 bar). It was found also that the welding current is the most influential parameter on weld quality. The best weld strength was obtained at 3.4 KA. Increasing welding current and welding time up to certain level increases the joint strength, after this level the joint strength decreases. Investigations showed also that the dominant structure of the nugget is martensite. The fracture due to tensile shear test was mainly intergranular in ferritic stainless steel side and the fracture mode was button pullout. Microhardness values recorded their highest values at locations where carbides existed beside the martensite of the nugget.
[M. El-Shennawy and S. M. Khafagy. **Parameters' Effect on Weld Quality for Dissimilar Spot Welding Between Ferritic Stainless Steel and Low Carbon Steel Sheets.** J Am Sci. 2012;8(5):100-107]. (ISSN: 1545-1003). http://www.americanscience.org. 14

Keywords: Spot welding; dissimilar welding; weld quality; controlling parameters; ferritic stainless steel; metallurgical and mechanical characteristics.

1. Introduction

Because of its high speed and adaptability for automation in high-rate production of sheet metal assemblies, resistance spot welding is widely used and applied in many industrial productions. It is also faster than arc welding or brazing and requires less skill to perform which make the process of resistance spot welding economical in many job shop operations [1]. Under the pressure of the requirements for lower cost and less weight of the products, dissimilar sheet metal assemblies are now being applied in automotive industries [2]. It is used for joining low carbon steel components for the bodies and chassis of automobiles, buses, trucks and office furniture [3–5].

Austenitic stainless steels and low carbon steels are welded similarly [6-7] and dissimilarly [8-9] by using resistance spot welding technique. Dissimilar welding between ferritic stainless steel and low carbon steel by using spot welding received limited attention and, therefore limited information about it is available. Ferritic stainless steel AISI 430 grade and low carbon steel were the dissimilar materials selected for this study. Effect of main welding parameters on weld quality of these steels has been studied. Those parameters included welding current, welding pressure (electrode force) and welding time. Weld quality was evaluated based mainly on weld strength. Therefore, microstructure investigation and microhardness and tensile shear examination for the dissimilar weld were carried out to determine the main spot welding parameters' effect on the weldability of ferritic stainless steel and low carbon steel sheets.

2. Materials and Experimental Methods

2.1. Materials and welding process

Two steel grades were used in this study; 430 grade ferritic stainless steel and low-carbon grade steel having 0.5 mm and 0.6 mm thickness, respectively. Chemical compositions and mechanical properties of both steels are given in Tables 1 and 2, respectively. Both materials were cut into pieces in dimensions of 150 mm x 25 mm. Sheet materials were spot welded using spot welding machine capable of 0–17.5 kA weld current. Welding was carried out by using water cooled conical electrode. Welding was performed by overlapping the plates linearly to fabricate the specimens for tensile shear test shown as schematically in Fig. 1. Various parameters were applied to examine their effects on weld quality as given in Table 3. The effect of welding current, applied pressure and welding time were the parameters investigated in this study. Fractured samples of the resistance spot dissimilar welded specimens after tensile shear test are shown in Fig. 2.

2.2 Mechanical testing and metallographic examination

Mechanical testing for spot welded specimens included tensile shear test and Vickers microhardness examination. Tensile shear test was carried out for all

spot welded specimens. Photos for tensile test experiments are presented in Fig, 3. Vickers microhardness for the spot, HAZ and base materials' regions of some selected specimens were determined. Metallographic examination included microstructure test for selected specimens using optical and scanning electron microscopes. Fracture surface examination was also carried out. Figure 3 illustrates the tensile process for a welded specimen.

Table 1 Chemical compositions for the raw materials used in the study.

Steel	C	Si	Mn	P	S	Cr	Mo	Ni
AISI 430	0.05	0.29	0.22	0.03	0.002	15.6	0.05	0.21
	Al	Co	Cu	Nb	Ti	V	W	Fe
	<0.001	0.02	0.29	0.007	0.003	0.09	0.023	83.13
Low-carbon steel	C	Si	Mn	P	S	Cr	Mo	Ni
	0.08	0.009	0.17	0.016	0.006	0.01	0.0016	0.014
	Al	Co	Cu	Nb	Ti	V	W	Fe
	0.112	0.007	0.004	0.0008	0.0006	0.004	0.02	99.54

Table 2 Mechanical properties for the raw materials used in the study.

Property / Steel	σ_T, MPa	0.2 %, σ_y, MPa	Elongation, %	ASTM Specification
AISI 430	450	205	22	**A 176, A 240**
Low-carbon steel	315	193	18	---

Table 3 Parametric analysis for the dissimilar spot welded joints.

Changing Parameter	Fixed parameters		Changing Parameter	Fixed parameters		Changing Parameter	Fixed parameters	
A, amp (x1,000)	P, MPa	T, cycle	T, cycle	P, MPa	A, amp (x1,000)	P, MPa	T, cycle	A, amp (x1,000)
2.5	0.2	6 & 10	2	0.2	3 & 3.4	0.14	6, 8 & 10	3 & 3.4
2.8			3			0.16		
3.0			5			0.18		
3.2			6			0.20		
3.4			7			0.22		
3.7			8			0.24		
A: Welding current, Amperage P: Welding pressure, MPa			10 11			T: Welding time, cycles 1 cycle = 0.02 sec.		

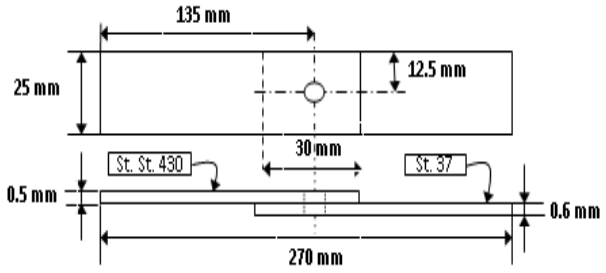

Fig. 1 Schematic representation for the dissimilar spot welded joint.

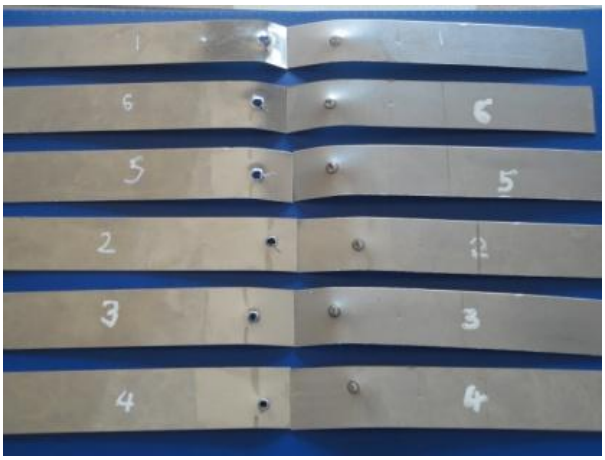

(a) Current effect

(b) Time effect

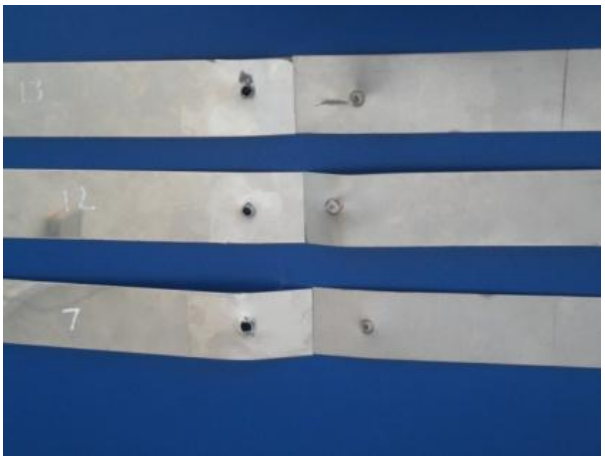

(c) Pressure effect

Fig. 2 Samples for dissimilar spot welded specimens after tensile shear test for different conditions.

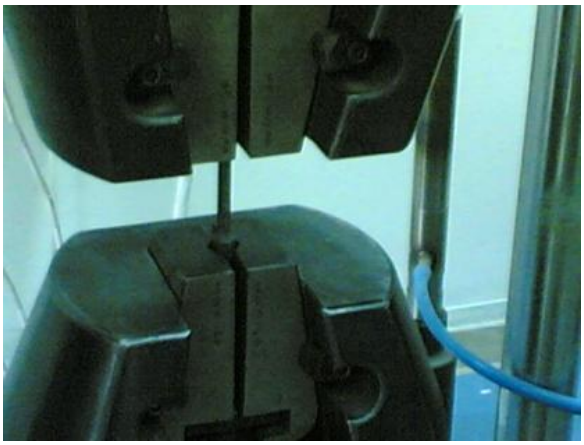

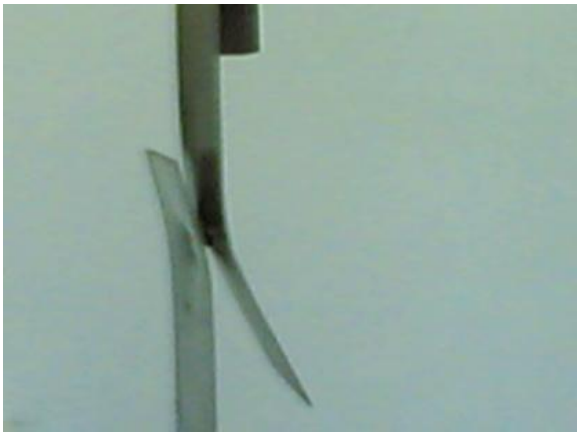

Fig. 3 Tensile test for the spot welded specimens.

3. Results and Discussion

3.1 Effect of welding pressure

The resistance R in the heat formula, $Q = I^2Rt$ where Q is heat generated, I is current applied and t is duration of current, is influenced by welding pressure through its effect on contact resistance at the interface between the workpieces. Welding pressure is produced by the force exerted on the joint by the electrodes [1]. Therefore, the welding pressure is considered as an indirect controlling parameter on heat generated. Its effect on weld strength has been discussed through the applications of various welding pressures and examining the resulted weld quality. Figure 4 shows the relationship between welding pressure and weld strength at various welding current and welding time values.

From Fig. 4, at welding current 3.4KA and welding time 10 cycles, there was an increase in fracture load with increasing welding pressure up to 0.2MPa (2 bar) then fracture load decreases with welding pressure increases to more than 0.2MPa. Increasing electrode pressure above certain value, in this case 0.2MPa, resulted in increasing contact area and hence decreasing the contact resistance which led to decreasing the heat generated at the interface. To compensate this decrease, welding current or welding time should be increased. Welding current was increased but failure in the specimens was noticed for such thicknesses and welding could not be carried out.

Effect of welding pressure on weld quality was investigated at different welding current and welding time values. The relation showed linear behavior when welding current was 3.0KA either with welding time 8 or 6 cycles. Pressure effect could be noticed when current reaches its optimum value, in this case 3.4KA.

Because of such result the pressure was kept constant at 0.2MPa for the rest of the experiments (welding joints). The relation between welding energy, using the previous formula of Q, and the fracture force showed that the best joint quality is obtained with welding pressure of 0.2MPa.

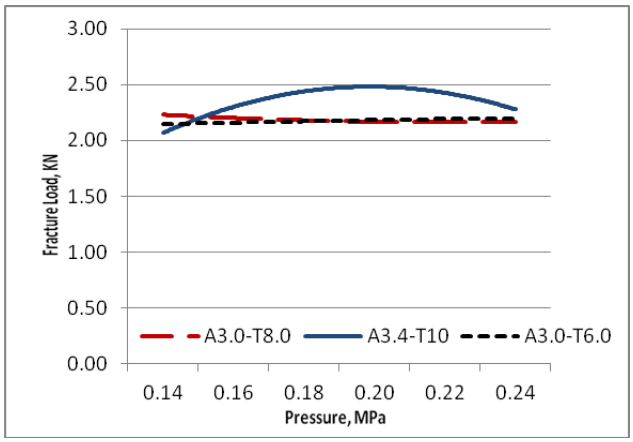

Fig. 4 Effect of welding pressure on fracture load.

3.2 Effect of welding current

Current is an important parameter to be controlled in the welding process because it has the greater effect on the generation of heat than resistance or time according to previous formula of Q, where I has the power of 2 in the equation. The pressure of welding electrode was fixed to 0.2MPa and various welding current values were applied to detect its effect on fracture load. Increasing welding current from 2.5KA to 3.7KA (the maximum possible applicable

current for this condition), the fracture load increases and reaches its maximum at welding current about 3.4KA which recorded 2.78KN and then decreases to 2.57MPa as shown in Fig. 5. Excessive current will cause molten metal explosion [10-11] as shown in Fig. 6 resulting in increasing the depth of indentation, which lower mechanical strength properties. This explains the decrease in the fracture load for specimens welded with current above 3.4KA.

Effect of welding current on weld strength has been investigated at lower welding time, 6 cycles. Direct linear relation is noticed between welding current and fracture load [12]. Decreasing welding time decreased the heat generated which affected the relation shown in Fig. 5.

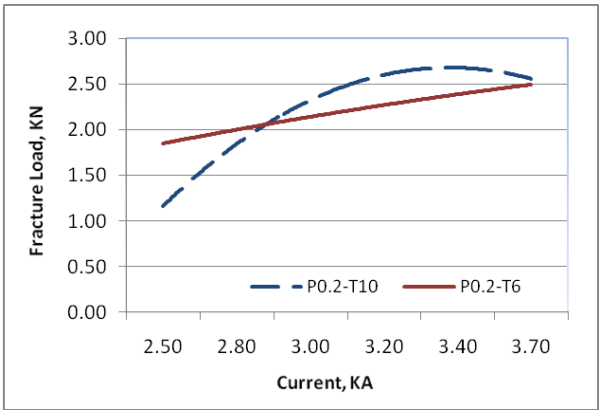

Fig. 5 Effect of welding current on fracture load.

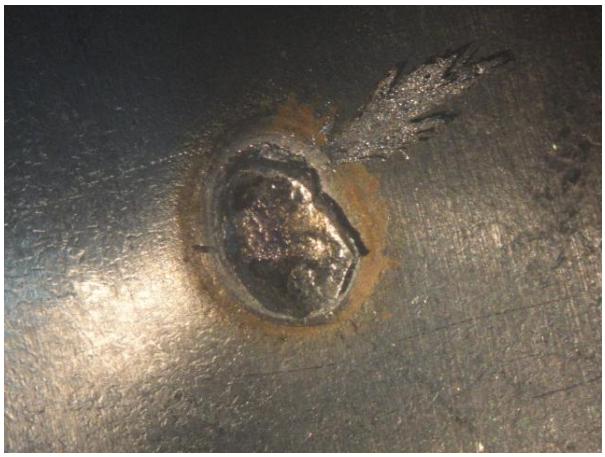

Fig. 6 Molten metal explosion from nugget.

3.3 Effect of welding time

Heat is lost by conduction into the surrounding base metal and electrodes; small amount is lost by radiation [1]. These losses increase with increases in weld time. Effect of welding time on fracture load has been investigated at two different welding current values of 3.0KA and 3.4KA. As shown in Fig. 7, at welding current 3.0KA increasing welding time from 2 cycles to 7 cycles results in fracture load increase [6] from 1.45 to 2.91KN. Extra increase in welding time from 7 cycles to 11 cycles decreases the fracture load to 2.2KN. Linear relation between welding time and fracture load is clearly seen in Fig. 7 for specimens welded with 3.4KA at different welding times.

It can be noticed that the maximum value for fracture load could be recorded with welding current 3.0KA and abt. 7 cycles welding time. This welding time is nearly 50% of that required to reach the same fracture load with welding current 3.4KA. At welding times of 4.5 and 8.5 cycles (the two intersecting points of the two curves in Fig. 7 fracture load for welded specimen either by 3.0 or 3.4KA is equal.

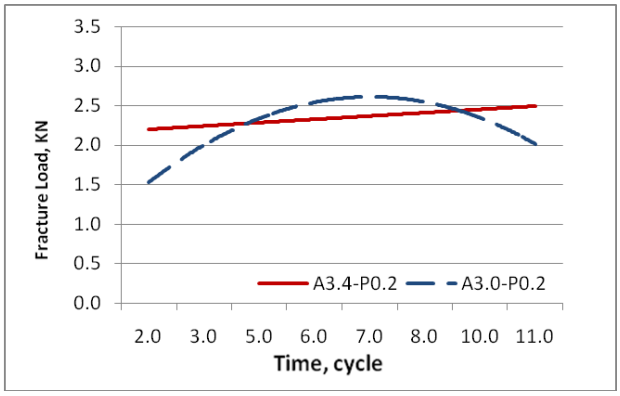

Fig. 7 Effect of welding time on fracture load.

3.4 Microstructure

In dissimilar metal welding, thermal conductivity and melting point are different. This will affect the melting time for each side of the resulted nugget in spot welded joint. Asymmetric nugget shape will be formed [7] as clearly shown in Fig. 8. The nugget size of FSS side of welded material is bigger than that of LCS side. Thermal conductivity of FSS is about half of that for LCS which helped in increasing temperature at FSS side. On the other hand, low carbon steel sheet has slightly thicker thickness compared to stainless steel sheet which promoted the cooling rate at carbon steel side resulting in lesser nugget size at this side.

Microstructure of the spot welded dissimilar joint was investigated using optical and scanning electron SEM microscopes. The microstructure of the HAZ of the FSS side is mainly consisting of two zones as shown in Fig. 9 (a). First zone is adjacent to fusion line which is large ferritic grains. Second zone is ferritic-martensitic structure. The martensitic is present along the ferrite grain boundaries [5, 8] and it is generally present as a continuous grain boundary phase as shown in Fig. 9 (b). It is also present as Ẅidmanstatten side plate that nucleate from the grain boundary and also from intergranularly as shown in Fig. 10. Thickness of each zone is dependent on the heat input (heat generated in welding). Increasing heat energy results in increasing first zone and decreasing the second one.

Decreasing heat generated in welding results in disappearance of the first zone totally and the second one became the dominant zone at HAZ of the FSS. It is worth mentioning that the specimen shown in Fig. 9 (b) where its welding current and time were 3KA and 8 cycles, respectively recorded fracture load of 2.13KN. And the specimen of Fig. 9 (a) where its welding current and time were 3.7KA and 10 cycles, respectively recorded fracture load of 2.57KN. It is apparent that the lesser heat generated resulted in lesser fracture strength.

The dominant HAZ structure of the nugget tip is ferritic structure with large grain size. This is observed for all welded specimens at different conditions as shown in Fig. 11.

At low carbon steel side the HAZ is gradually changing from martensitic structure adjacent to the fusion line to ferritic structure at the end of the HAZ with gradual decrease in grain size in the same direction as shown in Fig. 12. With increasing welding time, weld nugget will far exceed melting temperature and internal pressure may expel molten metal from nugget to adjacent HAZ with minute metal particles giving the shape of separated islands in some places at fusion line [10] as shown in Fig. 12.

Martensitic structure is the dominant structure in nugget zone. This is attributed to high cooling rate of this welding process. Carbides were also observed near fusion line of the FSS side as shown in Fig. 13. Dilution from FSS enhances the formation of carbides.

The mode of failure was button pullout [8, 13] as shown in Fig. 14. Investigating the fractured specimens after tensile shear test, it was noticed that the crack has been initiated from the nugget tip then propagated towards the FSS side [8] as shown in Fig. 15. Crack propagation was intergranular through the FSS grains as shown in Fig. 16. Microcracks were observed at the grain boundary of large ferritic grains as shown in Fig. 17. Microvoids were formed at the interface between the nugget and the formed layer in FSS side as shown in Fig. 15.

Fig. 8 Nugget macrostructure.

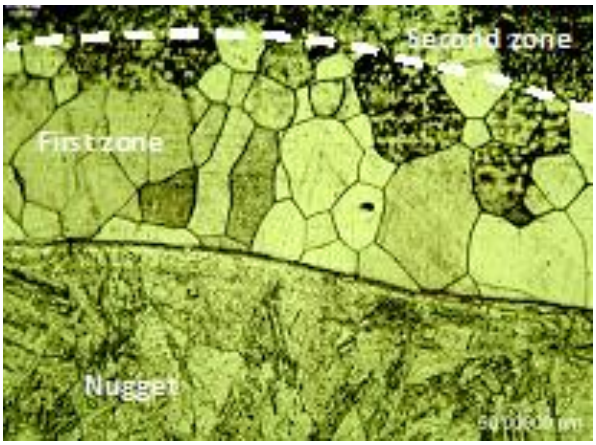

(a) I=3.7KA, t=10cycles.

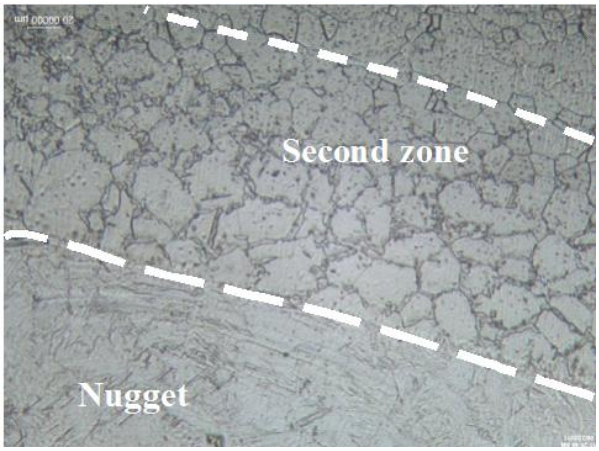

(b) I=3.0KA, t=8cycles

Fig. 9 Weld zone and HAZ for two different welded joints.

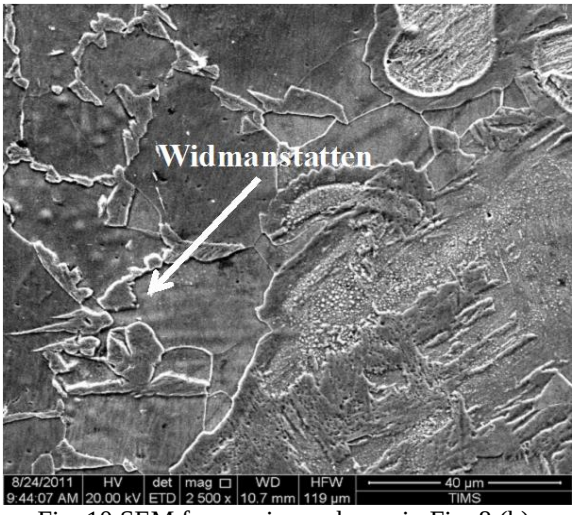

Fig. 10 SEM for specimen shown in Fig. 8 (b).

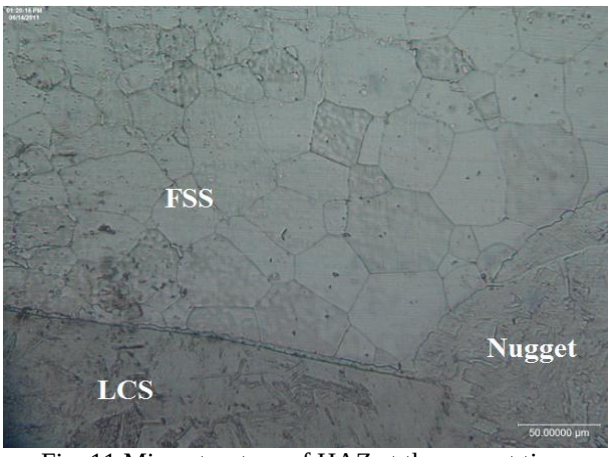

Fig. 11 Microstructure of HAZ at the nugget tip.

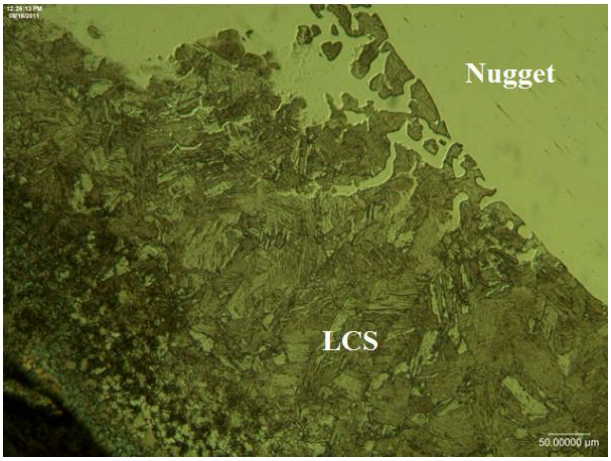

Fig. 12 Microstructure of the HAZ of low carbon steel side showing the separated islands. Welding conditions: I=3KA, t=8cycles.

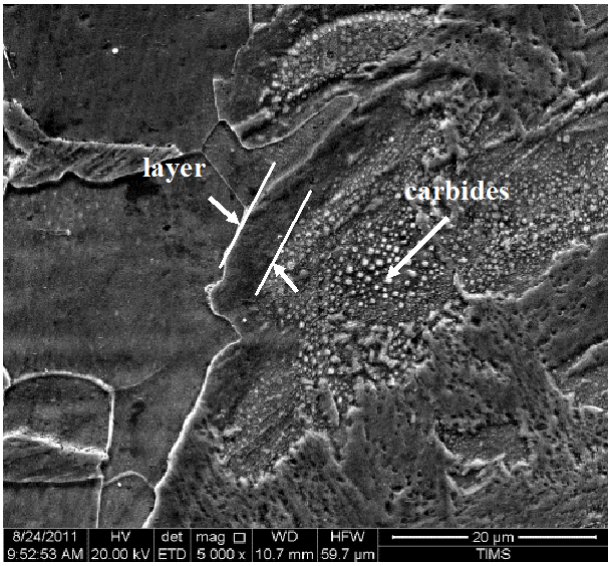

Fig. 13 Carbides formed and EDX distribution of alloying elements along formed layer at fusion line. Welding conditions: I=3KA, t=8cycles.

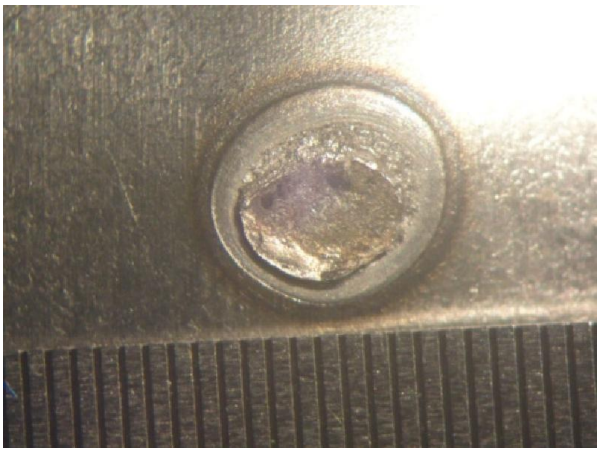
Fig. 14 Failure mode of dissimilar spot welded joint.

Microhardness

Microhardness measurements were carried out alongside the nugget, starting from one tip and ending at the other. Two parallel lines of measurements were taken as schematically shown in Fig. 18 (a). Figure 18 (b) shows two nearly similar profiles. The higher values are attributed to the martensitic structure formed in nugget zone [5, 8]. In the FSS side, the microhardness profile showed a little two peaks at the locations where the microstructure showed carbide formation. Variation in microhardness through joint thickness is shown in Fig. 18 (c). These results are in a good agreement with the last findings where the highest value of microhardness was recorded at the same places where the carbide formed shown in Fig. 13.

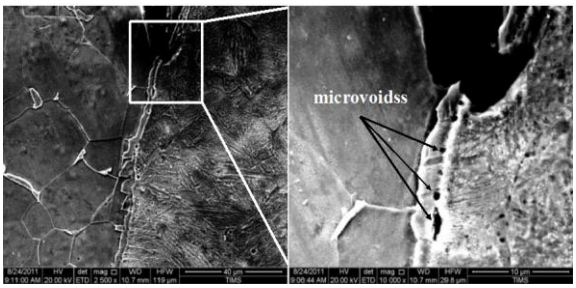

Fig. 15 Crack initiation after tensile shear test. I=3KA, t=8cy.

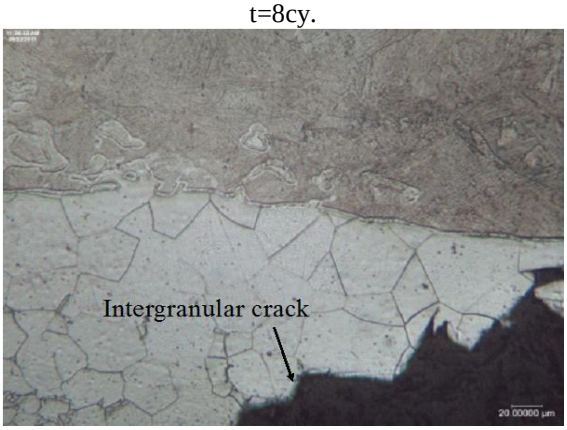

Fig. 16 Intergranular crack.

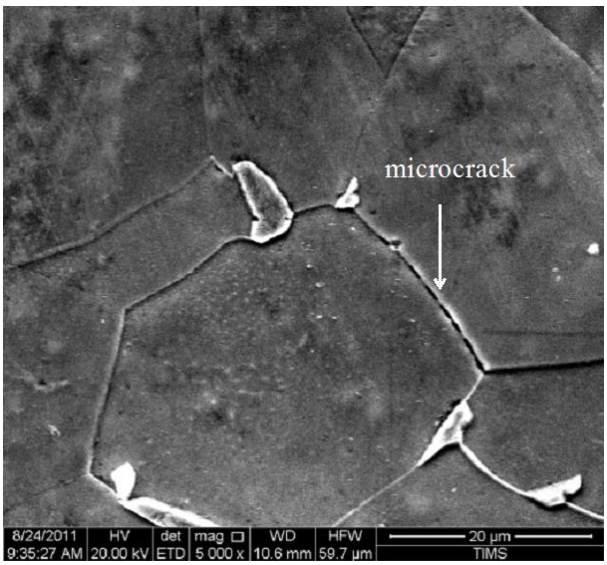

Fig. 17 Microcracks formed at large ferritic grains.

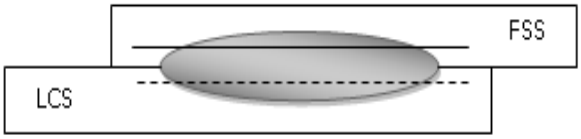

(a) Schematic diagram

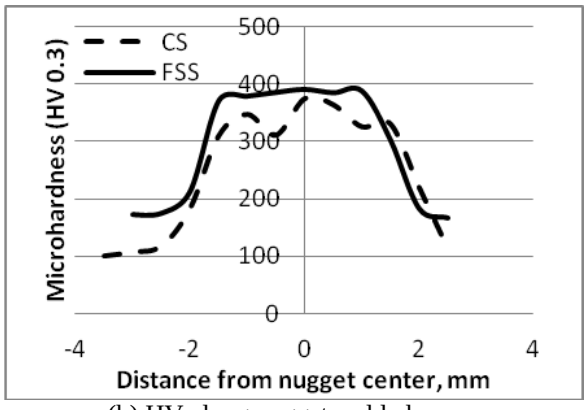

(b) HV along nugget welded zones

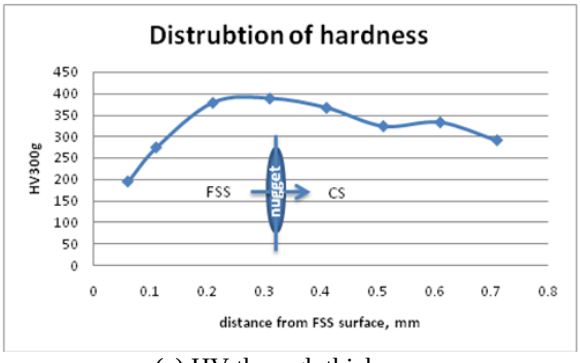

(c) HV through thickness

Fig. 18 Microhardness values for spot welded specimens at different locations, welding cond. I=3 KA, t=8cycles.

Conclusions

This work discusses the effect of main controlling parameters, welding current, welding time and electrode pressure, on the quality of spot welded dissimilar joint between ferritic stainless steel FSS sheet with 0.5 mm thickness and low carbon steel LCS sheet with 0.6 mm thickness. From the results of the study the following remarks can be drawn:

1. The suitable electrode pressure in this combination of steels was found to be 0.2MPa (2 bar).
2. Welding current is the most influential parameter on weld quality.
3. Increasing welding current and welding time improve the weld strength up to certain level after which the joint strength decreases.
4. The dominant structure of the nugget is martensite where the cooling rate is very fast in the spot welding process.
5. In tensile shear test, crack initiated at nugget tip and propagated intergranularly in HAZ of ferritic stainless steel side. Fracture mode was button pullout.
6. Microhardness values recorded their highest value at locations where carbides existed beside the fusion line.

Corresponding author:
M. El-Shennawy
Mechanical Engineering Department, Faculty of Engineering, Helwan University, Helwan, Cairo, Egypt
moha_111@yahoo.com.

References

1. Welding processes (1980): AWS welding handbook, 7th ed., vol. 3. London, England: American Welding Society, Macmillan Press Ltd.
2. Agashe S. and Zhang H. (2003): Selection of schedules based on heat balance in resistance spot welding. Welding J; 82 (7): 179S–183S.
3. Kaluc E. (1988): An effect of resistance spot welding parameters on the tensile shear strength and intergranular corrosion in the ferritic–austenitic stainless steels weldment. PhD thesis, Istanbul Technical University, Institute of Applied Science.
4. Norrish J. (1992): Advanced welding processes. Bristol, Philadelphia and New York, United Kingdom: Institute of Physic Publishing.
5. Vural M. and Akkus A. (2004): On the resistance spot weldability of galvanized interstitial free steel sheets with austenitic stainless steel sheets. J Mater Process Tech; 153–154: 1-6.
6. Kocabekir B., Koçar R., Gündüz S. et. al. (2008): An effect of heat input, weld

atmosphere and weld cooling conditions on the resistance spot weldability of 316L austenitic stainless steel, J Mater Proc Tech; 195: 327-335.
7. Haanbaşoğlu A. and Kaçar R. (2007): Resistance spot weldability of dissimilar materials (AISI 316L-DIN 10130-99 steels), J Mater & Design; 28: 1794-1800.
8. Marashi P., Pouranvari M., Amirabdollahian S. et. al. (2008): Microstructure and failure behavior of dissimilar resistance spot welds between low carbon galvanized and austenitic stainless steels, J Mater Sci & Engng A.; 480: 175-180.
9. Sun X., Stephens E. V., Khaleel M. A., et. al. (2004): Resistance spot welding of aluminum alloy to steel with transition material — from process to performance — Part I: Experimental study, Welding Journal; 83 (6): 188-s to 195-s.
10. Zhang H. and Senkara J. (2006): Resistance welding fundamentals and applications, CRC Press; 61-67.
11. Pouravari M., Mousavizadeh S. M., Marashi S. P. H et. al. (2011): Influence of fusion zone size and failure mode on mechanical performance of dissimilar resistance spot welds of AISI 1008 low carbon steel and DP600 advanced high strength steel, J Mater & Design; 32: 1390-1398.
12. Pereira A. M., Ferreira J. M., Loureiro A. et. al. (2010): Effect of process parameters on the strength of resistance spot welds in 6082-T6 aluminium alloy, J Mater & Design; 31: 2454-2463.
13. Hayat F. (2011): The effects of the welding current on heat input, nugget geometry, and the mechanical and fractural properties of resistance spot welding on Mg/Al dissimilar materials, J Mater & Design; 32: 2476-2484.

4/2/2012